JTTEE5 17:623–630
DOI: 10.1007/s11666-008-9221-1
1059-9630/$19.00 © ASM International



# In Situ Visualization of Impacting Phenomena of Plasma-Sprayed Zirconia: From Single Splat to Coating Formation

*Kentaro Shinoda, Hideyuki Murakami, Seiji Kuroda, Kohsei Takehara, and Sachio Oki*

*(Submitted May 13, 2008; in revised form August 26, 2008)*

**The authors have developed an in situ monitoring system for particle impacts under atmospheric dc plasma spraying conditions. This system utilized a high-speed video camera coupled with a long-distance microscope, and was capable of capturing the particle-impinging phenomena at one million frames per second. To understand the coating formation mechanism, two approaches were attempted, i.e., observation of the single splat formation and the subsequent coating formation. In the former case, the deformation and cooling processes of yttria-stabilized zirconia (YSZ) droplets impinging on substrates were successfully captured. In the latter case, multiple-droplet-impacting phenomena were observed as an ensemble treatment. Representing the coating process, the tower formation (0-dimensional) and bead formation (1-dimensional) were observed under typical plasma spray conditions for thermal barrier coatings using a triggering system coupled with the motion of a robot. The obtained images clearly showed the coating formation resulting from the integration of single splats.**

**Keywords** coatings for gas turbine components, diagnostics and control, influence of spray parameters, TBC topcoats

## 1. Introduction

Plasma spraying of yttria-stabilized zirconia (YSZ) has been widely used for thermal barrier coatings (TBC) on turbine blades. It can also be applied to solid oxide fuel cells (Ref 1, 2). It is important to understand the fundamental formation mechanism of plasma-sprayed coatings, which can be roughly classified into five regions: plasma jet formation, powder injection, particle heating and acceleration, single particle impact accompanying spreading and solidification, and coating formation by successive impact of particles. Based on the three-dimensional transient modeling work of arc root fluctuation (Ref 3) and in-flight particle diagnostics (Ref 4, 5), the three upstream processes are now well understood. On the contrary, the subsequent two phenomena, i.e., single splat and coating formations, have not been fully understood, especially due to the experimental difficulty. As a result, the process parameters could be related to the coating properties, e.g., adhesion strength, porosity, and crack density, only by the design of experiments such as the Taguchi method (Ref 6), leaving the impact processes in the state of black boxes. Although the Taguchi method itself is a strong tool for optimizing coating properties in industry, and although recent development in on-line control of spray processes enables the advanced evaluation utilizing in-flight particle characteristics, such as velocity and temperature, these parameters could be only optimized within the limitation of conventional plasma spray processes. In other words, if we can elucidate the splat formation and subsequent coating formation, we can reconstruct the plasma spray process from phenomenological aspects, which will then give us new insights into plasma spray technologies.

To observe these two processes, we need to estimate the characteristic time scale of the plasma spray process. As Vardelle and Fauchais summarized (Ref 7, 8), for a single splat formation, flattening and splashing occur within a few microseconds, followed by solidification within 10 μs; two successive impacts are on the order of 10-100 μs; one layer/pass, which is the unit of coating, is on the order of ms. Thus, the measurement system with the time resolution of less than 1 μs will be required to capture the single splat formation, while a system that can record the event for ms for the coating formation is needed.

This article is an invited paper selected from presentations at the 2008 International Thermal Spray Conference and has been expanded from the original presentation. It is simultaneously published in *Thermal Spray Crossing Borders, Proceedings of the 2008 International Thermal Spray Conference,* Maastricht, The Netherlands, June 2-4, 2008, Basil R. Marple, Margaret M. Hyland, Yuk-Chiu Lau, Chang-Jiu Li, Rogerio S. Lima, and Ghislain Montavon, Ed., ASM International, Materials Park, OH, 2008.

**Kentaro Shinoda, Hideyuki Murakami,** and **Seiji Kuroda**, Coating Materials Group, Composites and Coatings Center, National Institute for Materials Science (NIMS), 1-2-1 Sengen, Tsukuba, Ibaraki 305-0047, Japan; and **Kohsei Takehara** and **Sachio Oki**, School of Science and Engineering, Kinki University, 3-4-1 Kowakae, Higashi Osaka, Osaka 577-8502, Japan. Contact e-mail: shinoda.kentaro@nims.go.jp.

Meanwhile, Etoh et al. developed an image sensor for a high-speed video camera (HSV) based on the concept of "ISIS" (in situ storage image sensor) (Ref 9). It enables us to capture 100 consecutive images at 1 million frames per second (fps) with the exposure time of 250 ns. Recent progress in charge-coupled device ultrahigh-speed video cameras were reviewed by Thoroddsen et al. (Ref 10). This HSV may enable us to observe not only a single splat formation, but also the subsequent coating formation.

In this context, we have developed an in situ monitoring system utilizing the HSV of 1 million fps to capture the impacting phenomena during atmospheric dc plasma spraying (APS) (Ref 11). First, the impact phenomena of an YSZ droplet were observed by coupling the HSV with a long-distance microscope. The tower and bead formations were then observed using a triggering system coupled to the motion of a dc plasma torch to demonstrate the TBC formation.

## 2. Experimental

### 2.1 Single Splat Formation

Detailed descriptions and a schematic diagram of the developed in situ monitoring system are shown elsewhere (Ref 11, 12). A conventional dc plasma torch with a 40 kW subsonic anode (SG-100 with type 2083-165 anode, TAFA, Inc., A Praxair Surface Technologies, Inc.) was used as the APS system. A single particle was collected using a V-shaped roof-type shield with a hole and a single particle collector (Ref 13, 14).

An HSV (HPV-1, Shimadzu Corp., Japan) coupled with a long-distance microscope (QM100, Questar Corp.) was utilized to monitor the droplet impact. The pixel count and gray levels of the HSV at 1 million fps are 81,120 (= 312 in width × 260 in height) and 10 bits, respectively. The working distance and the angle between the substrate and the microscope were 11.4 cm and 31.4 degrees, respectively. Other optics to collect the thermal radiation history during impact were utilized as a trigger source for the HSV.

The experimental conditions are shown in Table 1(a). Hollow-oven spherical powder (HOSP) of 8-wt.%YSZ (204NS, Sulzer Metco Inc.) sieved to 45-53 μm was sprayed onto a quartz glass plate with the thickness of 0.5 mm. The substrate surface temperature was kept at 300 K during the experiments.

### 2.2 Coating Formation

We have tried to observe the formation of a tower by fixing a plasma torch (0 dimension, 0D), and the formation of a bead by scanning the plasma torch on a line (1 dimension, 1D). Experimental conditions for the 0D and 1D observations are shown in Table 1(b) and (c), respectively. The HOSP of the 8-wt.%YSZ (204NS sieved to 45-53 μm for 0D and 204B-NS, Sulzer Metco, for 1D measurements, respectively) were sprayed onto grit-blasted steel substrates (50 × 100 × 5 mm) with the dc plasma torch. The experimental conditions were designed so that they were identical to those under which the segment TBC could be formed, as shown in Table 1(d) (Ref 15, 16) except for the substrate temperature.

**Table 1 Experimental conditions at (a) single splat, (b) tower, and (c) bead formations; (d) reference conditions**

| Parameters | a, b, c | d(a) |
|---|---|---|
| Current, A | 800 | 800-1200 |
| Voltage, V | 32 | 32 |
| Primary gas, Ar, SLM(b) | 50 | 50 |
| Secondary gas, He, SLM | 13 | 13 |
| Powder feeding rate, g/min | 3, 7, 14 | 20 |
| Carrier gas, Ar, SLM | 8.5 | 8.5 |
| Spray distance, mm | 100(c) | 60-100 |
| Powder size, μm | −53, −53, −75/45 | −120/20 |
| Preheating temperature, K | 300 | 643-973 |
| Traverse speed, mm/s | 200, 0, 50 | 150-200 |
| Grit blasting | No, Yes, Yes | Yes |

(a) Guo et al. (Ref 15, 16); (b) SLM: standard liters per minute; and (c) a shield was inserted between the torch and the substrate

Prior to the coating formation observations, the flow rate, velocity, temperature, and size distributions of the in-flight particles were measured by an in-flight particle monitoring system (DPV2000, Tecnar Automation Ltd., Canada). The spray conditions were the same as the 1D measurement shown in Table 1(c).

For the 0D experiment, capturing of the images was conducted at arbitrary times. For the 1D experiment, a robot was programmed to scan the dc torch 10 times back and forth in the straight line, in which one scan of 50 mm length took 7 s including the wait time. A simple triggering system was constructed to trigger the HSV linked to the motion of the robot. The trigger timing was adjusted so that the HSV could record the impinging phenomena when the flow rate of the particles impinging on the center of the field of view (FOV) of the HSV became a maximum value, based on the result of the in-flight particle diagnostics. The substrate temperature was monitored using a k-type thermocouple inserted in the middle of the substrate.

## 3. Results

### 3.1 Single Splat Formation

Figure 1 shows the deformation and cooling processes of a droplet impinging on a substrate taken by the HSV. Each frame interval $t_I$ was 1 μs and the exposure time $t_E$ was 500 ns. From the images, this droplet was evaluated to be 50 μm in diameter and impacted on the substrate at a speed of 170 m/s. First, a sprayed droplet entered the FOV of the HSV from right to left in frame 1, and impinged on the substrate in frame 2. As soon as the droplet impinged on the substrate, a liquid sheet jetted out from the droplet to form a splat. At this stage, the splat was disk-shaped, although a part of the periphery began to be notched as

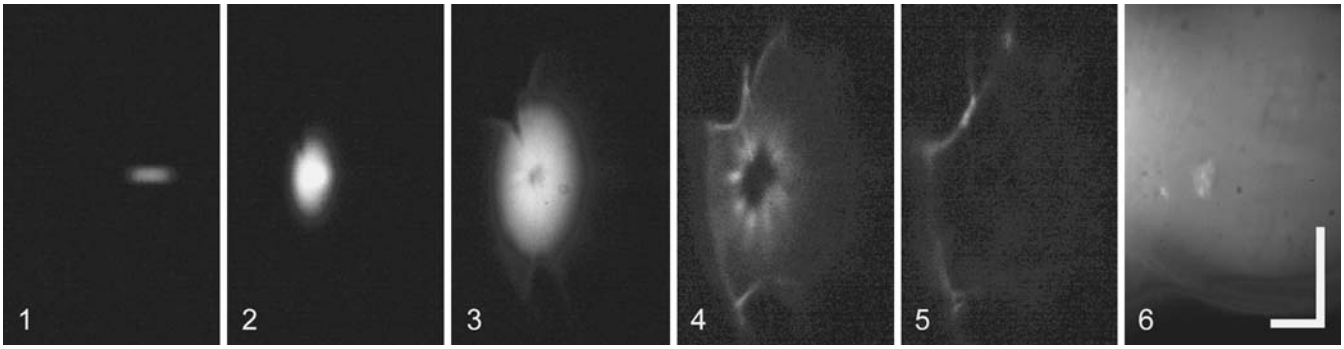


**Fig. 1** Thermal radiation images of a plasma-sprayed YSZ droplet impacting on a smooth cold quartz glass substrate (frames 1 to 5). Interval between each frame is 1 μs and exposure time of each frame is 500 ns. The resultant splat is shown in frame 6. Contrasts of the images were adjusted. The white scale bar indicates 200 μm in each direction on a substrate. Frames 1 to 5 were adapted with permission from Shinoda et al. (Ref 11)

observed in frame 2. The spreading sheet then started to slightly warp while the notch at the periphery was developing in frame 3. The center region of the splat already became darker than the surroundings, suggesting that this region experienced a more rapid cooling. In frame 4, the sheet became detached from the substrate and was still growing without disintegration. Detachment of the sheet can be judged by the asymmetry of the deforming splat on the both sides of the vertical centerline of the splat. Since the substrate was inclined against the HSV, the radius of the left hand side of the splat looks smaller than that on the right when detachment of the periphery occurs. Moreover, the rim could not maintain the disk shape, which indicates that the rim was no longer stable. The center part of the splat was far below the sensitivity of the HSV, which meant that it had already cooled at this stage. High-temperature regions were nonuniformly distributed along off-center. The detached sheet then began to rupture in frame 5. After rupture of the splat, only the central region was attached to the substrate as shown in frame 6.

### 3.2 In-Flight Particle Diagnostics

Figure 2 shows the in-flight particle distributions obtained by the in-flight particle monitoring system. The regions of $11 \times 35$ points with a 5 mm interval were measured. The measurement time for each point was 4 s. The trace of the maximum particle flow rate $R$ region was inclined to the x-axis; i.e., the maximum $R$ was leaving from the center with increasing the axial position $x$, suggesting that the injected powder penetrated the plasma jet and deviated from the central torch axis as was expected. The deviation angle off the x-axis, which was derived from the linear approximation, was 10.7 degrees. In the same manner, deviation angles of the particle temperature $T$, velocity $V$, and diameter $d$ were found to be 7.6, 6.7, and 11.9 degrees, respectively; i.e., the deviation became larger in the order of $V$, $T$, $R$, and $d$.

The radial position of the maximum flow rate zone, $y$, at $x = 100$ mm, was $-15$ mm. Therefore, when the torch was scanned in the direction of minus $y$ in the 1D observation, the HSV, which was focused at $x = 100$ mm, was triggered when the center axis of the torch reached 15 mm before the center of the FOV.

### 3.3 Coating Formation

Figure 3 shows the appearance of the obtained samples. When fixing the torch (0D), as was expected, a tower was formed. This tower was sprayed at the powder feed rate of 7 g/min for 186 s. The deposition region was 36 mm in diameter and the height of the tower was 21 mm. For a scanning torch (1D), a bead was formed. At the spray distance of 100 mm, the width and height of the bead were 19 mm and 607 μm, respectively. The reproducibility of the bead formation was relatively good so that the averaged bead width and thickness were approximately 20 mm and 600 μm for six time trials, respectively. This corresponds to the fact that the average thickness of 30 μm was deposited during each single pass. The substrate temperature during the 1D experiment increased from room temperature to 550 K during the bead formation.

Figure 4 shows the formation of a tower when fixing the torch (0D) as an example of the in situ observations. The tower was formed by the impact and deposition of particles. During the initial stage of the tower generation (a), the impacted particles isotropically splashed, because the impacted surface was flat. At (b), anisotropic particle splashing occurred, because the impacted plane formed a gradient according to the formation of the tower. At stage (c), the tower further grew and the top of the tower was out of the FOV. At any stage, the degree of splashing was greater at the center part of the tower, while the frequency of splashing decreased at the periphery of the tower. At the periphery, secondary particles were ejected and slowly flew in the radial direction. This can be the rebound phenomena of solid particles rather than the splashing of the liquids.

Bead formation was observed while scanning the torch on a line (1D). Since the scanning speed of the plasma torch was 50 mm/s, the motion of the torch during the video capturing was considered to be negligible. There were no obvious visual differences between the initial and

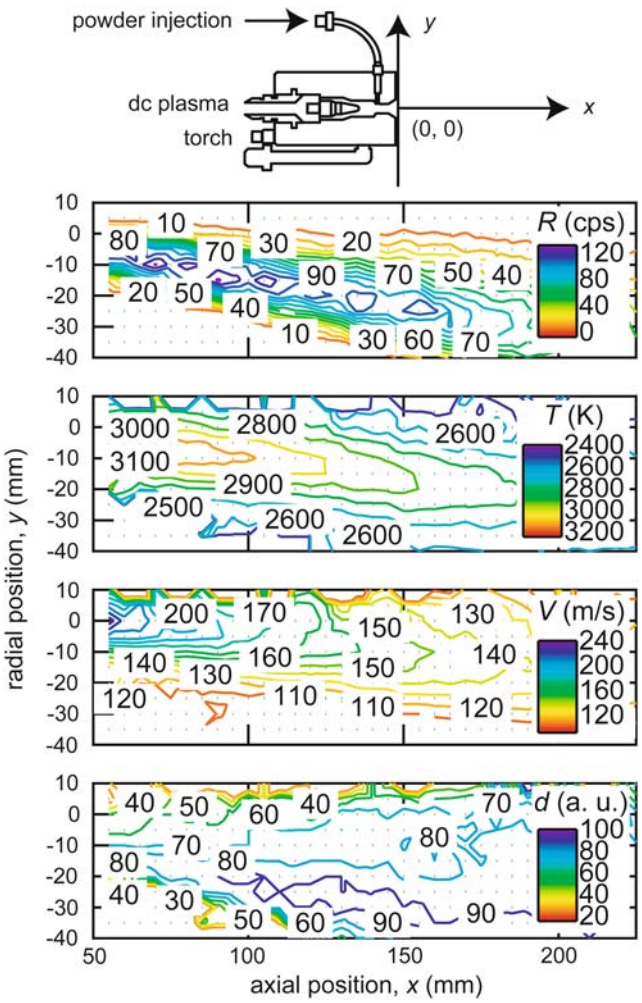


**Fig. 2** (color online) In-flight particle distributions concerning flow rate $R$ (counts/s (cps)), temperature $T$ (K), velocity $V$ (m/s), and diameter $d$ (arbitrary unit (a.u.)) on the axis of a dc plasma torch—that of particle injection port plane. The axial position $x$ (mm) is the distance from the head of the torch in the axial direction, and the radial position $y$ (mm) is the distance from the center of the torch perpendicular to the torch axis. The powder was injected from the plus side of the torch. The unit of $d$ is indicated not in meters but by a.u. due to the difficulty in calibration. The value of $R$ was derived from the number of particles that passed the measurement volume of an in-flight particle monitoring system divided by the measurement time

latter stages of the deposition. Hence, a detailed analysis of captured video was conducted. In this study, we showed the analyzed results for the first pass as the first step. Every particle that impacted the center region along the $y$-axis of the FOV in focus was captured, and the trajectory of the particle was tracked. From the trajectory, the velocity and impact angle to a substrate were derived as a function of the impact position in the direction of $y$. Figure 5 shows the relationship between these parameters. In the direction of the powder injection ($y$-axis), the velocity widely varied; the velocity reached 300 m/s when close to the center of the torch while 150 m/s when further from the torch. This means that the velocity difference was more than twice along the direction of the powder injection. The impact angle varied from 2 to 8 degrees according to the impacted position from the center to the further side. The velocity just before impact and the velocity during flight were almost the same, suggesting that in the case of plasma spraying, the existence of a substrate does not result in a significant deceleration of the particle.

Figure 6 shows the distribution of the particle impact velocity as a function of time. The velocity was distributed between 150 and 300 m/s, but occasionally exhibited narrow distribution (for instance $t \sim 400$ μs) where $180 < V < 220$ m/s. These results may be related to the plasma fluctuation, but a further investigation will be needed to confirm it.

Finally, Fig. 7 shows the cooling time of the impinged particle on a substrate as a function of the impact velocity. The cooling time was defined here as the time from which a particle impacted to when the brightness of the center of the impacting particle decreased to one-tenth, although this definition is not based on any physical model. Pearson's correlation coefficient $r$ between the cooling time and the impact velocity was −0.21, suggesting the tendency in which the cooling time decreased with the increase in the particle impact velocity.

## 4. Discussion

### 4.1 Coating Formation in Relation to Single Splat Formation

For single splat formation, interesting findings are that the center region of the splat had already cooled while the periphery was still spreading at a higher temperature. Assuming that the dynamic range of the HSV in temperature was 500 K, the cooling rates at the center and periphery were estimated to be 3-5 × $10^8$ and 5-10 × $10^7$ K/s, respectively. This means that the cooling rate at the center and that at the periphery would differ up to one order of magnitude. Thus, for the impact phenomena on a cold surface, the temperature distribution within a deforming droplet is not uniform, which cannot be disregarded. For the shape of a spreading droplet, McDonald et al. also captured similar images of YSZ droplets impacting on a cold smooth glass substrate: the droplets did not splash until they spread to the maximum spread extent (Ref 17). Our study was consistent with their images. However, their images lacked temperature information due to utilizing a short pulse laser as an illumination. The obtained thermal images contain complement temperature information to their shadow images.

We reported that the droplet spreading and splashing phenomena on a cold substrate in plasma spraying could be categorized as a splash between a prompt splash and a corona splash (Ref 11). According to previous studies (Ref 18-21), in the prompt splash, secondary droplets emerge and detach at the advancing liquid-substrate contact line. The corona splash is reminiscent of a crown. A symmetric corona is first formed, followed by secondary

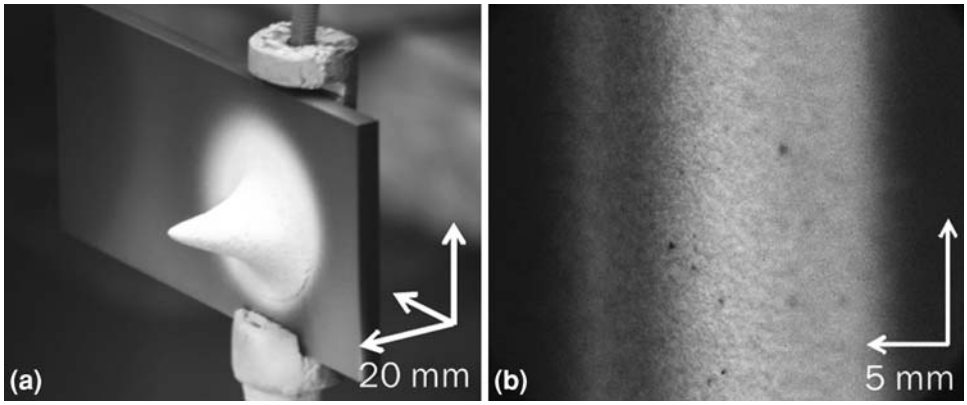


**Fig. 3** (a) Obtained tower and (b) bead at 0D and 1D measurements, respectively

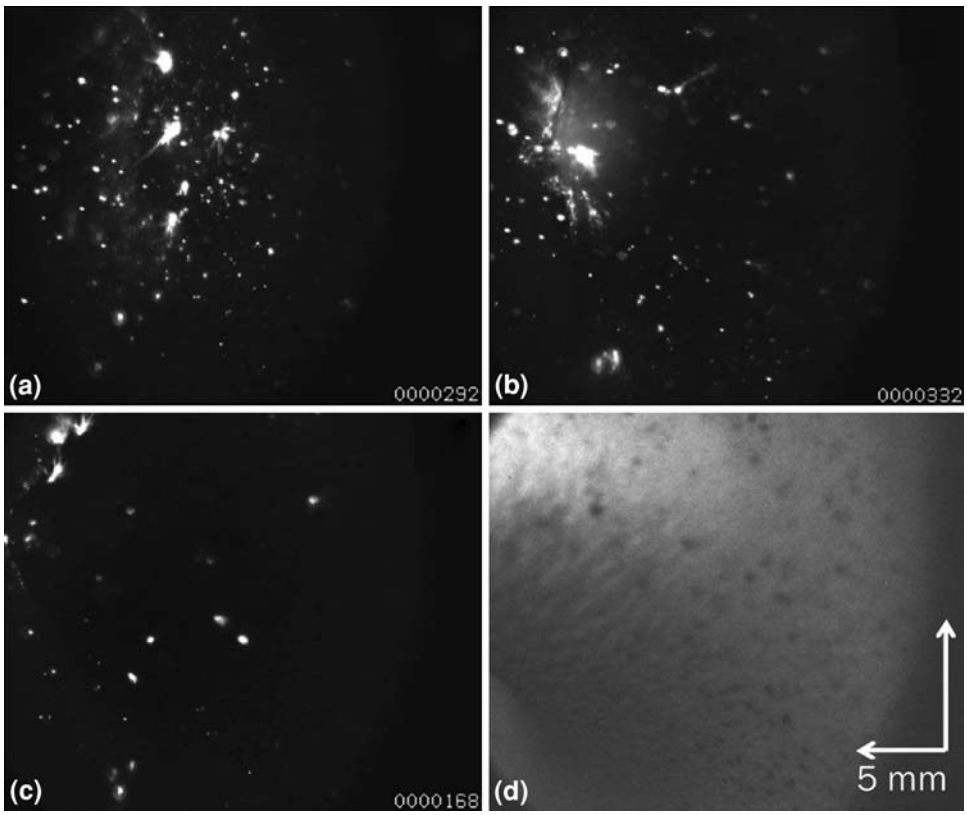


**Fig. 4** In situ observation of tower formation at fixing torch (0D): (a) 12 s, (b) 43 s, and (c) 64 s after powder injection. (d) After deposition. Monitoring was conducted at 43° from a substrate. The scale is for a substrate plane

droplets ejected from the expanding corona. In parallel to our previous research (Ref 11), Xu et al. gave simple and clear explanations to this matter. The prompt splash and corona splash are caused by the surface roughness and by instabilities produced by the surrounding gas, respectively (Ref 20, 21). In our observations, during the first splat formation on a cold smooth glass substrate, the droplet spread to its maximum extent without breakage, while on the actual surface of the tower and bead formations, particles splashed instantly after impact. In the latter case, the surface was considered not as smooth from the previously deposited layer. Thus, the splash on a cold smooth substrate in plasma spraying seemed as a type of corona splash, while the splash observed in the tower and bead formations appeared as the prompt splash.

### 4.2 Parameters Measured and to be Measured

In this study, we have measured the velocity and trajectory of impacting particles. For the comparison, the

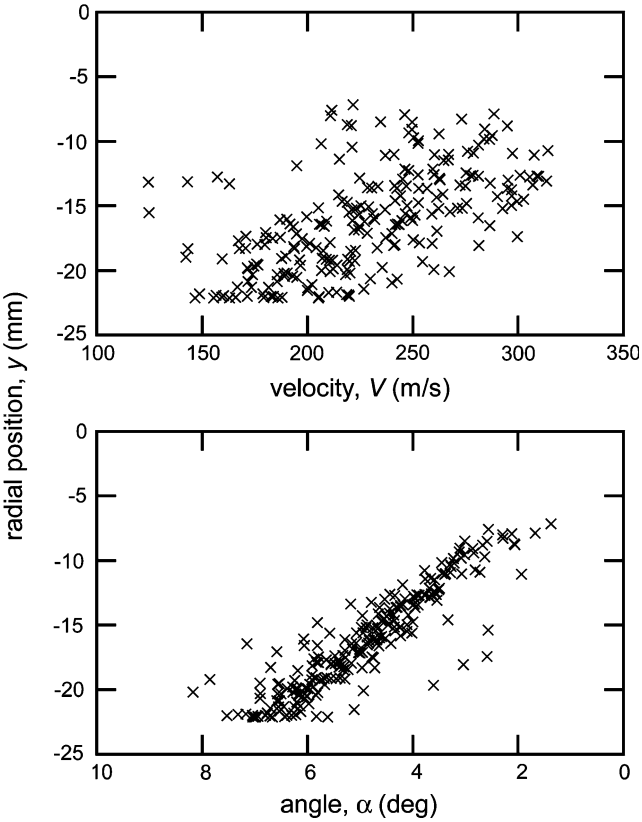


**Fig. 5** Particle impact velocity $V$ (m/s) and angle $\alpha$ (°) distributions along radial position $y$ (mm). Position $y$ (mm) is the distance from the center of the torch perpendicular to the torch axis. The powder was injected from the plus side of the torch

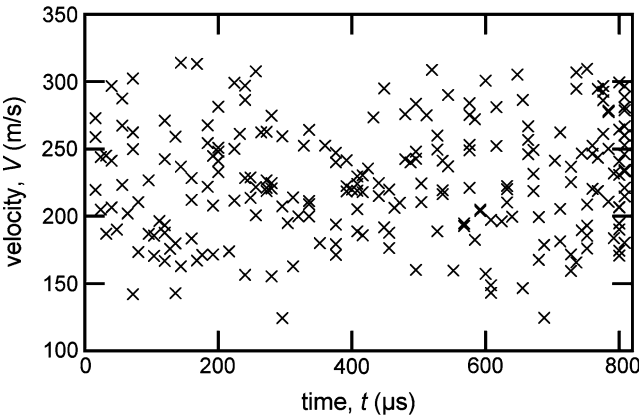


**Fig. 6** Time-resolved particle impact velocity $V$ (m/s). The time $t = 0$ corresponds to the start of recording of a high-speed video camera

velocity measured with the HSV was plotted with that measured with DPV2000 in Fig. 8. The velocity of the HSV tended to show the larger value than that of DPV2000; the velocity of the HSV was approximately 20% greater than that of DPV2000 at the maximum velocity at each position $y$; meanwhile, lower velocity

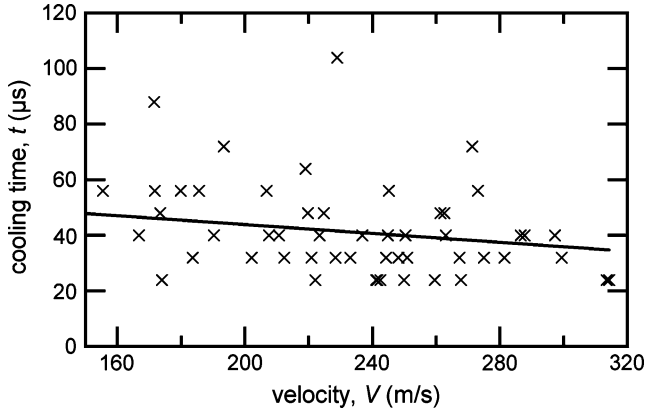


**Fig. 7** Relationship between particle cooling time $t$ (μs) and impact velocity $V$ (m/s)

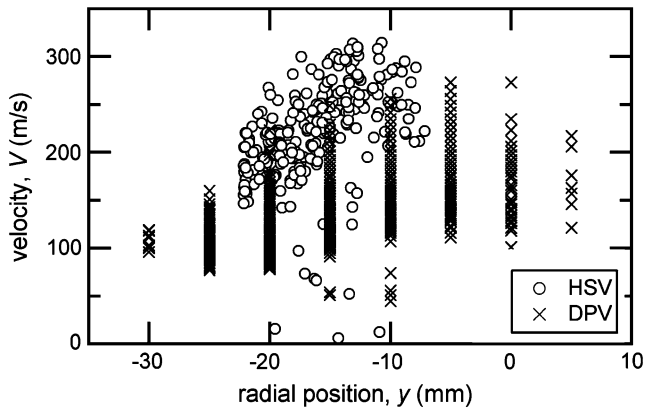


**Fig. 8** Comparison of impact velocity $V$ (m/s) derived from a high-speed video camera (HSV) with that measured with an in-flight particle monitoring system (DPV) as a function of radial position $y$ (mm). The position $y$ is the distance from the center of the torch perpendicular to the torch axis. The powder was injected from the plus side of the torch. The data of DPV was at the axial position of 100 mm

particles could not be detected with the HSV. Although there were such discrepancies in the absolute values, the tendency was consistent. The method to derive the velocity and trajectory was similar to particle imaging velocimetry, thus the results were also consistent with the phase Doppler particle anemometry as reported by Cetegen and Yu (Ref 22).

Since we did not measure the temperature in this study, we utilized the cooling time instead of the cooling rate for coating formation observations. The definition of the cooling time in this study was rather arbitrary and had no specific physical meanings. However, as Moreau et al. correlated the cooling time to the cooling rate, they will have an inverse relationship (Ref 23). Hence, our results in Fig. 7 suggested that increasing the impacting velocity increased the cooling rate of droplet. Since the impact velocity has a positive relation with the Reynolds number, the result was consistent with the previous study on a single splat by Vardelle et al. in which the increase in the Reynolds number increased the cooling rates (Ref 24).

We measured some parameters in situ, yet at least two other factors should be measured to understand the plasma spray process quantitatively. One is the molten degree of in-flight particles. From the previous study on the melting index (Ref 25), some portion of particles would not be fully molten when they reached to the substrate. Even with the precise surface temperatures, molten status inside droplets would not be known (Ref 26). The other is the degree of splashing. Most particles splashed during the coating formations, but even with recent advanced simulation model on the coating formation process the degree of splashing is left out (Ref 27). The experimental study to quantify the degree of splashing especially in volume fraction will be needed.

Last, we have showed the feasibility of direct observations on the coating formation process with the HSV including cases of the stationary plasma torch conditions (0D) and of the bead formation (1D). Since the bead is a unit of the coating, our approach is expected to form a basis to extend to the actual coating process in plane (2D) or in solid (3D).

## 5. Conclusion

In this study, we have tried to visualize two important phenomena during plasma spraying, that is, single splat formation and the subsequent coating formation. Utilizing the in situ monitoring system coupled with the HSV of 1 million fps enabled us to clearly capture the consecutive images of the deformation and cooling behavior of an YSZ droplet impinging on a cold smooth substrate: The liquid sheet jetting out sideways from the droplet became detached from the substrate and kept spreading without disintegration until its maximum extent; the center part of the flattened droplet rapidly cooled while the liquid sheet was still spreading. Representing a coating process, tower (0D) and bead (1D) formations were observed. The successive evaluation of the splat formations as a function of their impact position and time became possible. Particle impact velocities varied by two times along the direction of the powder injection. The cooling rate of the splats tended to become faster with increasing the impact speed.

### Acknowledgments

We thank Prof. Takehar-Goji Etoh (Kinki University) for his useful discussions. We also thank Mr. Masayuki Komatsu and Mr. Nobukazu Kakeya (NIMS) for help with the experiments.

### References

1. T. Yoshida, Toward a New Era of Plasma Spray Processing, *Pure Appl. Chem.*, 2006, **78**(6), p 1093-1107
2. F. Gitzhofer, M. Boulos, J. Heberlein, R. Henne, T. Ishigaki, and T. Yoshida, Integrated Fabrication Processes for Solid-Oxide Fuel Cells Using Thermal Plasma Spray Technology, *MRS Bull.*, 2000, **25**(7), p 38-42
3. E. Moreau, C. Chazelas, G. Mariaux, and A. Vardelle, Modeling the Restrike Mode Operation of a DC Plasma Spray Torch, *J. Therm. Spray Technol.*, 2006, **15**(4), p 524-530
4. J.F. Bisson, B. Gauthier, and C. Moreau, Effect of Plasma Fluctuations on In-Flight Particle Parameters, *J. Therm. Spray Technol.*, 2003, **12**(1), p 38-43
5. J.F. Bisson and C. Moreau, Effect of Direct-Current Plasma Fluctuations on In-Flight Particle Parameters: Part II, *J. Therm. Spray Technol.*, 2003, **12**(2), p 258-264
6. P. Saravanan, V. Selvarajan, M.P. Srivastava, D.S. Rao, S.V. Joshi, and G. Sundararajan, Study of Plasma- and Detonation Gun-Sprayed Alumina Coatings Using Taguchi Experimental Design, *J. Therm. Spray Technol.*, 2000, **9**(4), p 505-512
7. P. Fauchais, Understanding Plasma Spraying, *J. Phys. D: Appl. Phys.*, 2004, **37**, p R86-R108
8. A. Vardelle, C. Moreau, and P. Fauchais, The Dynamics of Deposit Formation in Thermal-Spray Processes, *MRS Bull.*, 2000, **25**(7), p 32-37
9. T.G. Etoh, D. Poggemann, G. Kreider, H. Mutoh, A.J.P. Theuwissen, A. Ruckelshausen, Y. Kondo, H. Maruno, K. Takubo, H. Soya, K. Takehara, T. Okinaka, and Y. Takano, An Image Sensor which Captures 100 Consecutive Frames at 1 000 000 Frames/s, *IEEE Trans. Electron Dev.*, 2003, **50**(1), p 144-151
10. S.T. Thoroddsen, T.G. Etoh, and K. Takehara, High-Speed Imaging of Drops and Bubbles, *Annu. Rev. Fluid Mech.*, 2008, **40**, p 257-285
11. K. Shinoda, H. Murakami, S. Kuroda, S. Oki, K. Takehara, and T.G. Etoh, High-Speed Thermal Imaging of Yttria-Stabilized Zirconia Droplet Impinging on Substrate in Plasma Spraying, *Appl. Phys. Lett.*, 2007, **90**(19), Art. No. 194103 (3 pp)
12. K. Shinoda, H. Murakami, S. Kuroda, S. Oki, K. Takehara, and T.G. Etoh, High-Speed Thermal Imaging of Yttria-Stabilized Zirconia Droplets Impinging on a Substrate in Plasma Spraying, *Proceedings of the 18th International Symposium on Plasma Chemistry*, K. Tachibana, Ed., August 26-31 2007 (Kyoto), International Plasma Chemistry Society, 2007, Art. No. 28C-a3 (4 pp)
13. K. Shinoda, Y. Kojima, and T. Yoshida, In Situ Measurement System for Deformation and Solidification Phenomena of Yttria-Stabilized Zirconia Droplets Impinging on Quartz Glass Substrate under Plasma Spraying Conditions, *J. Therm. Spray Technol.*, 2005, **14**(4), p 511-517
14. K. Shinoda, T. Koseki, and T. Yoshida, Influence of Impact Parameters of Zirconia Droplets on Splat Formation and Morphology in Plasma Spraying, *J. Appl. Phys.*, 2006, **100**(7), Art. No. 074903 (6 pp)
15. H.B. Guo, H. Murakami, and S. Kuroda, Effect of Hollow Spherical Powder Size Distribution on Porosity and Segmentation Cracks in Thermal Barrier Coatings, *J. Am. Ceram. Soc.*, 2006, **89**(12), p 3797-3804
16. H.B. Guo, S. Kuroda, and H. Murakami, Microstructures and Properties of Plasma-Sprayed Segmented Thermal Barrier Coatings, *J. Am. Ceram. Soc.*, 2006, **89**(4), p 1432-1439
17. A. McDonald, C. Moreau, and S. Chandra, Thermal Contact Resistance Between Plasma-Sprayed Particles and Flat Surfaces, *Int. J. Heat Mass Transfer*, 2007, **50**(9-10), p 1737-1749
18. R. Rioboo, C. Tropea, and M. Marengo, Outcomes from a Drop Impact on Solid Surfaces, *At. Sprays*, 2001, **11**, p 155-165
19. A.L. Yarin, Drop Impact Dynamics: Splashing, Spreading, Receding, Bouncing, *Annu. Rev. Fluid Mech.*, 2006, **38**, p 159-192
20. L. Xu, L. Barcos, and S.R. Nagel, Splashing of Liquids: Interplay of Surface Roughness with Surrounding Gas, *Phys. Rev. E*, 2007, **76**(6), Art. No. 066311 (5 pp)
21. L. Xu, Liquid Drop Splashing on Smooth, Rough, and Textured Surfaces, *Phys. Rev. E*, 2007, **75**, Art. No. 056316 (8 pp)
22. B.M. Cetegen and W. Yu, In-Situ Particle Temperature, Velocity, and Size Measurements in DC Arc Plasma Thermal Sprays, *J. Therm. Spray Technol.*, 1999, **8**(1), p 57-67
23. C. Moreau, M. Lamontagne, and P. Cielo, Influence of the Coating Thickness on the Cooling Rates of Plasma-Sprayed Particles on a Substrate, *Surf. Coat. Technol.*, 1992, **53**, p 107-114

24. M. Vardelle, A. Vardelle, A.C. Leger, P. Fauchais, and D. Gobin, Influence of Particle Parameters at Impact on Splat Formation and Solidification in Plasma Spraying Processes, *J. Therm. Spray Technol.*, 1995, **4**(1), p 50-58
25. L. Li, A. Vaidya, S. Sampath, H.B. Xiong, and L.L. Zheng, Particle Characterization and Splat Formation of Plasma Sprayed Zirconia, *J. Therm. Spray Technol.*, 2006, **15**(1), p 97-105
26. G. Mauer, R. Vassen, and D. Stover, Detection of Melting Temperatures and Sources of Errors Using Two-Color Pyrometry During In-Flight Measurements of Atmospheric Plasma-Sprayed Particles, *Int. J. Thermophys.*, 2008, **29**(2), p 764-786
27. R. Ghafouri-Azar, J. Mostaghimi, S. Chandra, and M. Charmchi, A Stochastic Model to Simulate the Formation of a Thermal Spray Coating, *J. Therm. Spray Technol.*, 2003, **12**(1), p 53-69